H_2-induced structural evolution in non-crystalline rhodium nanoparticles

Robert Choukroun,*[a] Dominique de Caro,[a] Bruno Chaudret,[a] Pierre Lecante[b] and Etienne Snoeck[b]

[a] *Laboratoire de Chimie de Coordination du CNRS (UPR 8241), 205, route de Narbonne, 31077 Toulouse cedex 4, France. E-mail: choukrou@lcctoul.lcc-toulouse.fr*
[b] *CEMES-LOE-CNRS, 29, rue Jeanne Marvig, BP 4347, 31055 Toulouse cedex, France*

Received (in Montpellier, France) 15th November 2000, Accepted 15th January 2001
First published as an Advance Article on the web 15th March 2001

A THF solution of $[Rh(\mu\text{-}Cl)(C_2H_4)_2]_2$ reacts in the presence of poly(vinylpyrrolidone) (PVP) with the 15-electron complex vanadocene, $[V(C_5H_5)_2]$, to give PVP-protected native rhodium particles. High resolution electron microscopy (HREM) and wide angle X-ray scattering (WAXS) experiments confirm the presence of a non-periodic structure (polytetrahedral atomic organization); when exposed to hydrogen, the rhodium particles exhibit a pattern consistent with the signature of a fcc lattice.

Rhodium is widely encountered in the fields of homogeneous (molecular complexes) and heterogeneous catalysis (alumina- or silica-supported particles). At the frontier between homogeneous and heterogeneous catalysis, small rhodium particles in colloidal suspensions are presently of great interest.[1] Colloidal dispersions of rhodium are at present nearly exclusively prepared by reduction of rhodium trichloride with chemical reducing agents such as dihydrogen,[1a,c,d] trisodium citrate,[1b] alcohols or ethers,[1e] and alkaline borohydrides.[1f,g] We have recently demonstrated the capability of vanadocene, $V(C_5H_5)_2$, to reduce $FeCl_2$ into nanoscale α-Fe^0.[2] The ability of vanadocene to react with chloride anions to give stable $V(C_5H_5)_2Cl$ and $V(C_5H_5)_2Cl_2$ species is expected to provide the driving force to reduce Rh^I to Rh^0 and we describe here an organometallic route to polymer-protected rhodium colloids from di-μ-chlorotetrakis(ethylene)dirhodium(I)[3] using highly reactive 15-electron vanadocene as reducing agent.

In a preliminary experiment, we showed that reaction of $[Rh(\mu\text{-}Cl)(C_2H_4)_2]_2$ with $V(C_5H_5)_2$ in THF led to a fine rhodium(0) powder, isolated as a black precipitate, which is flammable in air. A change in the colour of the solution from purple to blue indicated the oxidation of $V(C_5H_5)_2$ to $V(C_5H_5)_2Cl$.

The reaction of a THF solution of $[Rh(\mu\text{-}Cl)(C_2H_4)_2]_2$ with 2 equiv. $V(C_5H_5)_2$ in the presence of poly(vinylpyrrolidone) (K30-PVP, average molecular weight: 40 000) as protecting polymer at room temperature leads to rhodium colloids dispersed in PVP, isolated as the black solid [Rh-PVP] (Scheme 1).

The product can be easily purified by washing several times with THF to eliminate $V(C_5H_5)_2Cl$ and, possibly, unreacted $V(C_5H_5)_2$. The presence of vanadium and chloride impurities (less than 1%, see Experimental) was checked by elemental analysis and EDX. The solid is soluble in alcoholic and chlorinated solvents as well as in water, but is insoluble in aliphatic and aromatic solvents. To ensure that no ethylene remained chemisorbed on the surface of the nanoparticles, ^1H NMR experiments were carried out. It is well known that rhodium nanoparticles are able to hydrogenate olefins and we proposed to hydrogenate the residual C_2H_4 left in the catalyst, using ^1H NMR to detect any formation of ethane. The [Rh-PVP] nanoparticles (42×10^{-5} mol Rh) in suspension in deuterated benzene were stirred for 1 day under 6 bar H_2. The ^1H NMR spectrum of the solution (free C_2H_6 expected at δ 0.79) as well as mass spectrometric analysis of the gas phase above the solution do not show any formation of ethane. As a standard and for comparison, hydrogenation of a highly dilute solution of $[Rh(\mu\text{-}Cl)(C_2H_4)_2]_2$ (1.0×10^{-5} mol Rh) in deuterated benzene was performed under the same experimental conditions (1 day under 6 bar H_2). The ^1H NMR spectrum of the solution, under the same experimental conditions as above, shows a peak at δ 0.79 characterised as due to ethane {as a probe, higher concentrated solutions of $[Rh(\mu\text{-}Cl)(C_2H_4)_2]_2$ in C_6D_6 with H_2 give formation of C_2H_6}. This experiment also allows an evaluation of the detection limit of the ethane by comparison with the integration of the C_6D_5H signal used as a standard. Bearing in mind that the most frequently encountered size for rhodium nanoparticles (see histogram below) is nearly 1.1 nm, that is an ideal cluster of 55 atoms, it can be shown that 76% of rhodium atoms are on the surface, corresponding to nearly 32×10^{-5} mol Rh. At this stage, we estimate that less than 3% of rhodium atoms are linked to ethylene.

$$[Rh(\mu\text{-}Cl)(C_2H_4)_2]_2 + 2\ V(C_5H_5)_2$$
$$\xrightarrow[\text{THF, 298 K, 15 h}]{\text{K30-PVP}}$$
$$2\ [Rh_{colloids}\text{–PVP}] + 2\ V(C_5H_5)_2Cl + 4\ C_2H_4$$

Scheme 1

The low magnification TEM micrograph of the solid shows that the particles appear to be connected [Fig. 1(a)]. The HREM micrograph in Fig. 1(b) confirms the connections between the grains and evidences fringes in the particles. However, no regular periodicity is observed, which does not allow us to determine any periodic structure within the particles.

Structural characterisation of the rhodium colloids by wide angle X-ray scattering (WAXS) was performed in the solid state using procedures previously validated for colloids in PVP.[4] The radial distribution function (RDF) exhibits a set of well-defined peaks (Fig. 2, curve a) characterised however by a relatively broad first peak and a rapid dampening: no oscillation can be observed above 1.0 nm, suggesting a lack of long-range organisation. From the position of the first peak, the shortest bond length can be estimated to be 0.274 nm and clearly attributable to the metal–metal bond. This is direct evidence of the absence of significant oxidation of the sample. It also indicates that the impurities known to be present in the sample do not generate a signal strong enough to be detected beside the scattering from the rhodium particles, since this signal would correspond to significantly smaller distances. It

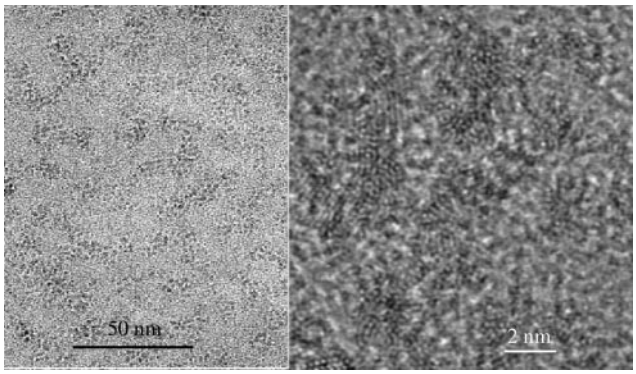

Fig. 1 (a) Low magnification TEM micrograph showing the dispersion of the rhodium nanoparticles. (b) HREM micrograph revealing the connections between the rhodium particles and the absence of a recognisable structure.

should be noted that this first distance is nearly 2% longer than in the bulk metal and also that the experimental RDF cannot be related to any simple lattice, which confirms the observations obtained by HREM. Of special interest is the lack of any peak at the $a\sqrt{2}$ distance, where a is the shortest metal–metal distance (0.269 nm for fcc rhodium). This feature is related to the presence of octahedral sites for the metal atoms inside the structure and can be observed in all compact structures.[5] Consequently, its absence and the observed splitting of the second peak in reciprocal space (not presented) indicate a drastic change in the local symmetry of rhodium. In previous studies on platinum colloids, whose bulk also crystallises in the fcc structure,[6] a well-defined pattern clearly related to the bulk structure was observed even for very small particles, and the bond length was found to be significantly shorter than in the bulk. A similar non-periodic order was observed in very small cobalt particles and could be related to a polytetrahedral atomic organisation.[7] When exposed to CO, the particles retain their structure and size (Fig. 2, curve b). However, the mean bond length is further increased to 0.283 nm, 5% longer than in bulk metal. It should be noted that all distances are linearly increased, which is consistent with the previously observed relaxation effect induced by CO coordination on the surface of metallic particles.[8]

The same batch of particles, when exposed to H_2, exhibits a very different pattern (Fig. 2, curve c) which is indeed quite consistent with the signature of a fcc lattice. We can observe that the coherence length is also close to 1.0 nm for the hydrogenated colloid. A simulated reduced intensity function can be computed using Debye's formula applied to a proposed model

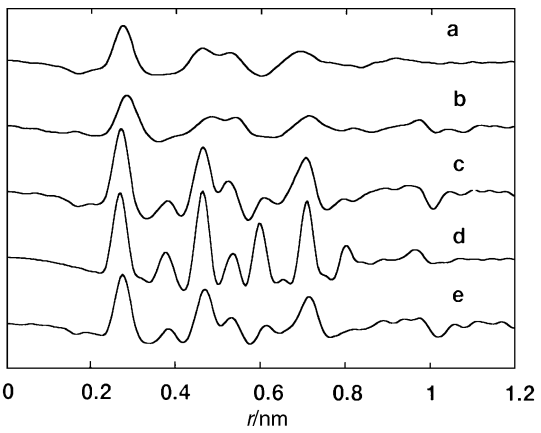

Fig. 2 WAXS RDF of (a) rhodium particles, (b) rhodium particles after exposure to CO, (c) rhodium particles after exposure to H_2, (d) simulation of a 55-atom cuboctahedron, (e) rhodium particles after exposure to H_2 + CO.

consistent in size and structure, in this case a small 55-atom cuboctahedron. A Fourier transform of this function then provides a simulated RDF, which can be compared to the experimental one (Fig. 2, curve d). The mean metal–metal distance needs to be adjusted to 0.266 nm, which indicates a contraction of approximately 1% compared to the bulk. The agreement is good enough to confirm the fcc lattice inside the particles: all distances generated by the model match peaks in the RDF. However, discrepancies can be observed regarding the amplitudes, and the experimental pattern is significantly broader than the simulated one, which is not the case for a perfect cuboctahedron. This might indicate deviations from the cuboctahedral shape and network distortions.

Finally, the same measurement procedure was applied to the hydrogenated colloids after further exposure to CO (Fig. 2, curve e). The RDF pattern remains consistent with a fcc structure, the coherence length being unchanged (1.0 nm). However, here also all the peaks are linearly shifted to larger values. The mean metal–metal distance is relaxed to 0.270 nm, very close to the bulk value, which is also consistent with the previously observed higher electron-donor character of CO *vs.* H_2.[8–10] The infrared spectrum of the hydrogenated colloid after exposure to carbon monoxide in methanol solution shows two CO bands at 1909(m) and 2027(s) cm^{-1} (Fig. 3, spectrum a), respectively attributed to bridging and linear CO on rhodium. For example, Mucalo and Cooney have observed two CO absorptions at 1900 and 2040 cm^{-1} for 4 nm poly(vinyl alcohol)-protected rhodium hydrosols.[1f] Our infrared spectrum is also very similar to that of CO adsorbed on evaporated rhodium films.[11] It should be noted that the infrared spectrum of rhodium colloids under CO is much more complex and shows six absorptions at 1846(w, br), 1977(m), 1995(sh), 2020(s), 2040(s) and 2066(w) cm^{-1}, for which we cannot provide assignments. Bubbling oxygen (60 min) over a sample exhibiting spectrum a results in the total disappearance of adsorbed CO bands (Fig. 3, spectrum b) due to the oxidation of chemisorbed CO to CO_2 as evidenced by mass spectrometry. This reaction has been widely encountered on supported rhodium nanoparticles.[12] In order to complete the study of rhodium colloids after H_2 and CO exposure, HREM experiments have been performed. Fig. 4 shows very well dispersed particles and clearly evidences the fcc structure of the Rh particles, as observed in the insert of Fig. 4. The histogram in Fig. 5 shows a relatively narrow size distribution for the particles, with a mean diameter of about 1.3 nm.

In conclusion, this study demonstrates that innovative chemical methods allow the preparation of very small rhodium nanoparticles with a narrow size distribution. These particles display a non-periodic polytetrahedral structure significantly less compact than the bulk. Such a structure may be induced by a size effect and/or the presence of impurities at the surface (*e.g.* residual vanadium oxides). Further activation of the particles with hydrogen leads to the bulk fcc structure of rhodium. This structural evolution could be associated with the full reduction of the surface of the particles in agreement

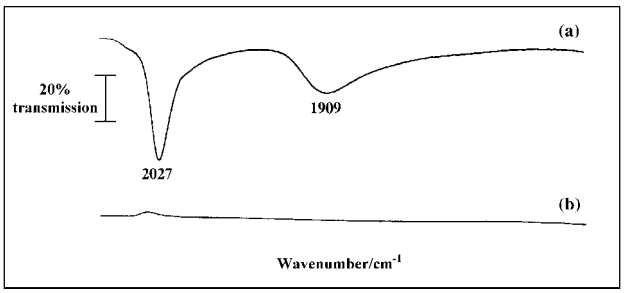

Fig. 3 Infrared spectra in the ν_{CO} stretching region: (a) CO adsorption on H_2-pretreated rhodium colloids in methanol solution; (b) after bubbling O_2 over a sample showing spectrum a.

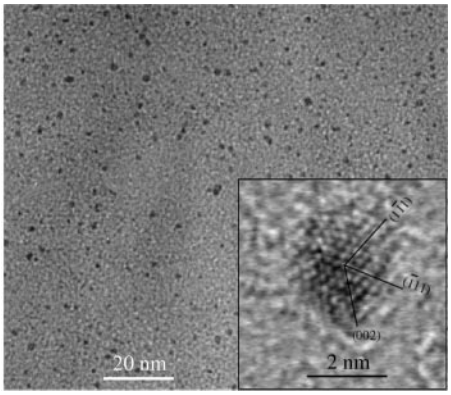

Fig. 4 Low magnification TEM micrograph showing the sizes of well-dispersed rhodium nanoparticles Insert: HREM micrograph evidencing the fcc structure of H_2-pretreated rhodium particles after reaction with CO.

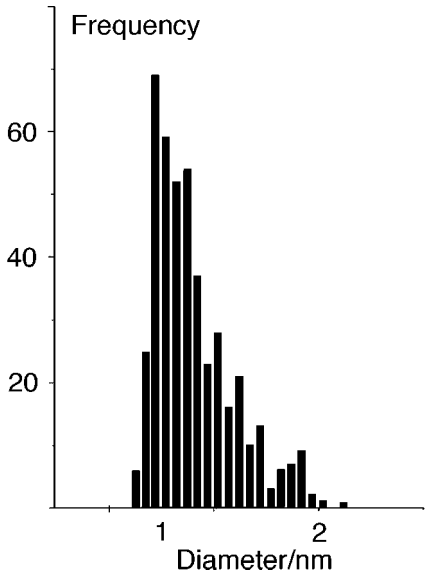

Fig. 5 Histogram of the Rh nanoparticle diameters. The mean diameter is 1.3 nm with a standard deviation of 0.4 nm from a sample population of 442.

with the contraction of the metal–metal distance observed in these nanoparticles. In addition, either H_2 diffusion into the Rh lattice or H_2-induced reconstruction as an adsorbed layer cannot be excluded. The study of the surface reactivity and the catalytic properties of these nanoparticles is presently in progress and will be presented elsewhere.

Experimental

The synthesis was carried out under an inert Ar atmosphere in a glovebox, typically as follows: a solution of $V(C_5H_5)_2$ (170 mg, 0.94 mmol) and K30-PVP (800 mg) in 20 mL THF was transferred into a solution of $[Rh(\mu\text{-}Cl)(C_2H_4)_2]_2$ (175 mg, 0.90 mmol of Rh metal) in 10 mL THF (initial weight ratio Rh : PVP = 11.5 wt%). The resulting solution was stirred for 15 h, during which time PVP-protected rhodium colloids precipitated from the solution and were isolated by filtration. The black solid thus obtained was washed several times with THF and finally dried (500 mg, elem. anal.: Rh = 9.7, V = 0.8, Cl = 0.5 wt%). After work-up of the THF filtrate of the solution, Cp_2VCl was fully characterised by CH elemental analysis and ^1H NMR.

A 1.0 mL aliquot of a deuterated benzene solution of $[Rh(\mu\text{-}Cl)(C_2H_4)_2]_2$ (1.0×10^{-5} mol Rh, prepared from a 10-fold concentrated solution) was left at room temperature for 24 h under 6 bar H_2. The ^1H NMR spectrum was collected and shows the formation of ethane [free C_2H_6: $\delta = 0.79$; ratio $C_6D_5H : C_2H_6$ (1H : 12H) was nearly 150]. A suspension of nanoparticles [Rh-PVP] (420 mg, *i.e.* nearly 42 mg Rh content or 4.2×10^{-4} mol Rh) in 1.0 mL of deuterated benzene was stirred at room temperature for 24 h under 6 bar H_2. The gas phase analysed by MS and the ^1H NMR spectrum of the solution do not show any formation of ethane (the same experimental parameters were used for collecting ^1H NMR spectra at 200 MHz). Additionally, the thermal decomposition of [Rh-PVP] (42 mg, *i.e.* 4.2 mg Rh content) under helium was carried out. A coupled MS analysis of the gas phase does not show any formation of C_2H_4.

TEM samples were prepared by slow evaporation in a glovebox of one drop of a dilute solution of the product in methanol deposited on a carbon-coated copper grid. Reproducible HREM images were obtained on samples produced from independent syntheses. The experiments were performed on a Philips CM 30/ST operated at 300 kV with a point resolution of 0.19 nm. The size distribution was measured through the numerical analysis of low magnification images TEM. In this procedure, the different particles were first identified according to an upper and lower intensity threshold, then counted and measured. HREM images of isolated particles were digitised at a resolution of 0.03 nm $pixel^{-1}$ and analysed using their numerical diffractograms (Fourier transforms). Solid samples for WAXS experiments were introduced into thin-walled Lindemann capillaries of 1.5 mm diameter, in a glove box filled with argon; the capillaries were sealed for the experiments. Measurements were carried out as previously described.[10] Data were normalised to one rhodium atom. Reproducible WAXS patterns were obtained on samples produced from independent syntheses. Infrared spectra were recorded in solution (methanol, *ca.* 3.9 mg mL^{-1} of metal) on a Perkin–Elmer FT-IR spectrophotometer. The reference spectrum of methanol was subtracted.

References

1 (*a*) H. Bönnemann, G. Braun, W. Brijoux, R. Brinkmann, A. Schulze Tilling, K. Seevogel and K. Siepen, *J. Organomet. Chem.*, 1996, **520**, 143; (*b*) G. Schmid, V. Maihack, F. Lantermann and S. Peschel, *J. Chem. Soc., Dalton Trans.*, 1996, 589; (*c*) K. S. Weddle, J. D. Aiken III and R. G. Finke, *J. Am. Chem. Soc.*, 1998, **120**, 5653; (*d*) T. Yonezawa, T. Tominaga and D. Richard, *J. Chem. Soc., Dalton Trans.*, 1996, 783; (*e*) H. Hirai, Y. Nakao and N. Toshima, *J. Macromol. Sci.-Chem. A*, 1979, **13**, 727; (*f*) M. R. Mucalo and R. P. Cooney, *Chem. Mater.*, 1991, **3**, 1081; (*g*) J. Schulz, A. Roucoux and H. Patin, *Chem. Commun.*, 1999, 535; (*h*) C. Larpent, E. Bernard, F. Brisse-Le Menn and H. Patin, *J. Mol. Catal.*, 1997, **116**, 277; (*i*) G. Schmid, in *Clusters and Colloids*, ed. G. Schmid, VCH, Weinheim, 1994, pp. 178–211; (*j*) H. Bönnemann and W. Brijoux, in *Active Metals*, ed. A. Fürstner, VCH, Weinheim, 1996, pp. 339–376.
2 R. Choukroun, D. de Caro, S. Matéo, C. Amiens, B. Chaudret, E. Snoeck and M. Respaud, *New J. Chem.*, 1998, **22**, 1295.
3 R. Cramer, *Inorg. Synth.*, 1974, **15**, 14.
4 M. Bardaji, O. Vidoni, A. Rodriguez, C. Amiens, B. Chaudret, M.-J. Casanove and P. Lecante, *New J. Chem.*, 1997, **21**, 1243.
5 (*a*) B. W. Van De Wall, *J. Non-Cryst. Solids*, 1995, **189**, 118; (*b*) J. P. K. Doyle and D. J. Wales, *J. Chem. Soc., Faraday Trans.*, 1997, **93**, 4233.
6 M.-J. Casanove, P. Lecante, E. Snoeck, A. Mosset and C. Roucau, *J. Phys. III*, 1997, **7**, 505.
7 F. Dassenoy, P. Lecante, M.-J. Casanove, M. Verelst, E. Snoeck, T. Ould Ely, C. Amiens and B. Chaudret, *J. Chem. Phys. B*, 2000, **104**, 695.
8 F. Dassenoy, K. Philippot, T. Ould Ely, C. Amiens, P. Lecante, E. Snoeck, A. Mosset, M.-J. Casanove and B. Chaudret, *New J. Chem.*, 1998, **22**, 703.
9 B. Moraweck and A. J. Renouprez, *Surf. Sci.*, 1981, **106**, 35.
10 A. Rodriguez, C. Amiens, B. Chaudret, M.-J. Casanove, P. Lecante and J. S. Bradley, *Chem. Mater.*, 1996, **8**, 1978.
11 R. Quéau and R. Poilblanc, *J. Catal.*, 1972, **27**, 200.
12 F. Solymosi, in *Nanoparticles in Solids and Solutions*, ed. J. M. Fendler and I. Dékány, Kluwer Academic Publishers, New York, 1996, pp. 407–419.